Baghdad Science Journal

Volume 23 | Issue 6 Article 11

6-22-2026

Effect of CuPc Film Thickness Prepared by Thermal Evaporation on the Performance of an Optical Detector

Zainab Hazim Abdul Raheem
Department of Physics, College of Science for Women, University of Baghdad, Baghdad, Iraq,
zainab.h@csw.uobaghdad.edu.iq

Sameer Khudhur Yaseen
Department of Physics, College of Science for Women, University of Baghdad, Baghdad, Iraq,
mohammed.k.khalaf@src.edu.iq

Mohammed K. Khalaf
Scientific Research Commission, Baghdad, Iraq

How to Cite this Article

Raheem, Zainab Hazim Abdul; Yaseen, Sameer Khudhur; and Khalaf, Mohammed K. (2026) "Effect of CuPc Film Thickness Prepared by Thermal Evaporation on the Performance of an Optical Detector," *Baghdad Science Journal*: Vol. 23: Iss. 6, Article 11.
DOI: https://doi.org/10.21123/2411-7986.5325

BAGHDAD SCIENCE JOURNAL 2026;23(6):2093–2104

Scan the QR to view the full-text article on the journal website

RESEARCH ARTICLE

Effect of CuPc Film Thickness Prepared by Thermal Evaporation on the Performance of an Optical Detector

Zainab Hazim Abdul Raheem [1], **Sameer Khudhur Yaseen** [1,*], **Mohammed K. Khalaf** [2]

[1] Department of Physics, College of Science for Women, University of Baghdad, Baghdad, Iraq
[2] Scientific Research Commission, Baghdad, Iraq

ABSTRACT

Copper phthalocyanine (CuPc) is a semiconductor that is chemically very stable, highly optically absorbing of visible light, and possesses good charge transport properties, so it is a promising material for optoelectronic devices and photodetectors. In this study, CuPc thin films with thickness range 146.4–632.4 nm were grown on ultrasonically cleaned glass substrates by thermal evaporation at a pressure of 2.2×10^{-5} torr. Structure, morphology, and optical properties were analyzed to study the effect of thickness on photoconductive response. X-ray diffraction analysis revealed that the films were polycrystalline monoclinic with preferred (312) orientation. AFM images showed increase in grain size with thickness, and roughness decreased at higher thicknesses due to increased surface density. Absorption spectra showed distinct Q and B regions, and the energy gap was observed to increase from 1.60 to 2.92 eV with increased thickness. Dark and illumination current–voltage curves showed Schottky-type behavior, indicating the existence of a potential barrier across the metal–semiconductor junction that is responsible for the charge transport. The photodetector device made from CuPc thin films also exhibited a good optical response with a quantum efficiency (η) value of 10.89%, responsivity (R) value of 0.054 A/W, and specific responsivity (D*) value of 10^9 Jones when illuminated with 625 nm. These findings corroborate that CuPc films exhibit thickness-dependent optical and electrical characteristics and are good prospects for stable high-performance Schottky-type photodetector applications.

Keywords: AFM, CuPc, PVD, UV- Visible, X-ray diffraction

Introduction

Copper Phthalocyanine (CuPc) is a conjugated macrocyclic organic semiconductor material that has gained a lot of interest in recent years due to its excellent chemical stability, high optical absorption, and wide electronic flexibility.[1] Its structure facilitates effective charge transport and intermolecular π–π interaction and is thus a very good prospective material for application in organic electronics, photovoltaics, and sensor devices.[2] In addition, CuPc has excellent photochemical and electrochemical stability so that it can be used effectively at ambient conditions,[3] which is extremely crucial in low-cost, flexible, and green electronic systems design.[4] Organic or inorganic semiconductors like silicon or CuPc are the driving components of modern electronics.[5] Inorganic semiconductors exhibit high mobility and charge reliability, but corresponding organic semiconductors like CuPc are highly flexible, light fabrication weight, and compatible with low-temperature, large-area processing.[6] Organic materials have gained considerable attention in recent years owing to their diverse applications in microelectronics, integrated

Received 29 June 2025; revised 28 October 2025; accepted 9 December 2025.
Available online 22 June 2026

* Corresponding author.
E-mail addresses: zainab.h@csw.uobaghdad.edu.iq (Z. H. Abdul Raheem), dr.sameerkhdeer.phy@gmail.com (S. K. Yaseen), mohammed.k.khalaf@src.edu.iq (M. K. Khalaf).

https://doi.org/10.21123/2411-7986.5325

circuits, and optoelectronic devices. These materials exhibit strong interactions with light due to high oscillatory strength, and their optical properties can be notably altered depending on their surrounding environment.[7] Copper phthalocyanine (CuPc) is an organic compound commonly used as an active layer in quartz crystal microbalance (QCM) applications for gas detection due to its remarkable chemical and thermal stability. Additionally, the presence of a phenyl group in the phthalocyanine structure enhances its ability to interact with various gases, including volatile organic compounds.[8] Phthalocyanine (Pc) thin films possess significant optical characteristics, including electrochromic and photovoltaic properties, making them suitable for the development of high-performance photophysical, conductive, photoconductive, and optoelectronic devices due to their 18 p-electron aromatic macrocyclic structure.[9] Organic semiconductors are essential to optoelectronic devices, extensively studied for their capacity to alter properties through chemical structural modifications and their ease of fabrication into flexible films and devices. Phthalocyanins (PCs), being organic compounds with substantial cyclic structures, have garnered significant interest from researchers owing to their exceptional physical and chemical properties.[10] Copper phthalocyanines (CuPcs) are recognized as organic semiconductors that enhance stability and boost the performance of organic display panels due to their role in charge injection. They have been extensively studied both theoretically and experimentally in recent years.[11] While solution processing methods are technologically simple, they effectively spread components evenly throughout the final film while maintaining precise control over its thickness. Hence, solution-processing methods generate significant attention in the fields of science and technology. Significantly, drop-casting, dip-coating, spin-casting, and spray-coating stand out among the various techniques. The use of drop-casting in industrial settings is limited due to the restricted coating area it can produce and the challenges associated with managing the deposition process. Nevertheless, this technique is beneficial for surface preparation, especially in the context of biomaterials and nanoparticles.[12] Phthalocyanines show promise in gas sensing, solar cells, color filters, electrophotography, security printing, optical logic displays, and sensitizers. These substances usually function as p-type semiconductors, which has the advantage of being comparatively stable in the presence of heat and chemicals. They are easily sublimed, producing thin, high-quality films that do not decompose. The physicochemical properties can be altered by altering the metal ion. The characteristics of the films in this organic semiconductor prototype are influenced by the substrate temperature, evaporation rate, and post-evaporation annealing procedure. This paper focuses on the optical analysis of thin films made from lead and copper phthalocyanine.[13] These materials have broad applications, including in solar cells,[14] organic dyes, gas sensor applications, photodiodes,[8] photoconductivity, material science, and even optical nonlinear behavior,[15] and so on. Recently, the structural, optical, and electronic properties of CuPc have been investigated by various factors, including annealing, concentration, and thickness.[16] The major objective of the current research work is to investigate how film thickness affects the structure, morphology, optical, and electrical properties of copper phthalocyanine (CuPc) thin films formed by thermal evaporation method. Particular emphasis is placed on identifying how changes in thickness affect photoconductive performance, Schottky-type I–V characteristics, and general optical detector performance in terms of quantum efficiency, responsivity, and detectivity. The ultimate goal is to determine the most favorable CuPc film thickness that provides the highest detection sensitivity and stability for applications in optoelectronic devices.

Materials and methods

The CuPc blue pigment, characterised by the molecular formula (C32H16N8Cu), was utilised in the investigation and procured from SIGMA-ALDRICH CHEMICAL with a purity of 99%. The powder is blue and has been employed as a raw material. Before initiating the deposition process, the substrate was cleaned, and various thicknesses of CuPc thin films were deposited using the thermal evaporation technique. The glass substrates were cleaned sequentially in an ultrasonic bath using acetone, ethanol, and deionized water for 10 minutes each to ensure the removal of organic and particulate contaminants. The film deposition was carried out under a high vacuum of approximately 2×10^{-5} Torr at room temperature.

Thin film deposition process

The deposition technique utilises vacuum thermal evaporation technology, wherein copper phthalocyanine undergoes heating to the point of evaporation and subsequently condenses on a cooled substrate, forming a thin coating. A coating apparatus capable of attaining high vacuums of up to 2×10^{-5} Torr was utilised. The dimensions of the deposition basin are symmetrical and geometric, including the target or base. This design enables the even distribution

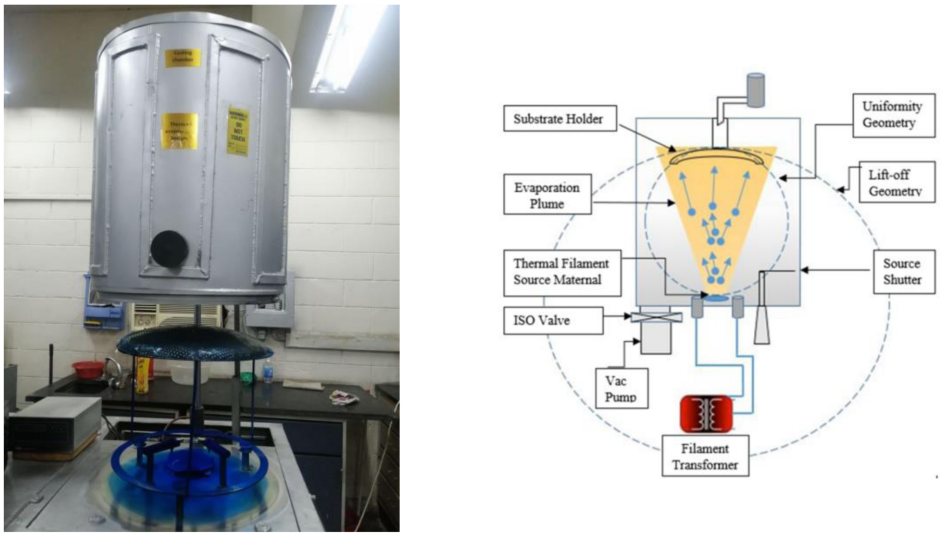

Fig. 1. Thermal evaporation system diagram.

of evaporated CuPc molecules on the substrate. The principal objective is to establish a uniform and constant coating of CuPc. Consistency in the deposited film is essential for attaining the requisite characteristics and specifications.

Fabrication of copper phthalocyanine films

Copper phthalocyanine films with thicknesses of 146.4, 232.2, 478.4, and 632.4 nm were produced within a molybdenum metal boat during the pressure of the evaporation chamber attained $2.2 \times 10^{(-5)}$ Torr, utilising a coating unit. At ambient temperature, the coating apparatus applied the material onto the glass located 30 cm from the evaporation chamber. A current transformer delivers a substantial current for deposition purposes. Subsequently, the samples are cooled in the evaporation chamber and prepared for thickness measurement. The laboratory then evaluates the structural, optical, morphological, and electrical properties of these films, as illustrated in Fig. 1. which shows the thermal evaporation system diagram.

Characterization

The samples were deposited using thermal evaporation, yielding four distinct thicknesses. The analysis utilised a JASCO UV-visible absorption spectrophotometer, operating within a wavelength range of 300 to 1100 nm. For the XRD analysis, we employed the SHIMADZU XRD-6000 system, with Cu K as the X-ray source. We employed Cu-Kα radiation, characterised by a wavelength of 1.78 Å, to acquire the diffraction pattern. The scanning occurred for 20 minutes inside the 20–90° range at a rate of 0.02° per minute, with a viewing time constant established at two. A 200 keV ultra-resolution scanning electron microscope (JEOL-2010) was employed to create the grids for FE-SEM research, facilitating the observation and documentation of the nanoparticles' size, shape, and organisational structure.

Results and discussion

X-ray diffraction

The XRD patterns of the films deposited at different thicknesses (146.4, 232.2, 478.4, and 632.4 nm) reflect a clear thickness dependence of crystallinity and texture. In the thinnest thickness (146.4 nm), the presence is noted of a broad, moderate-intensity XRD peak corresponding to the (312) plane, indicative of the presence of relatively large surface grains with poor crystallographic coherence. This broadening shows that the growth is of island-like mode (Volmer–Weber type) where discrete crystallites form on the substrate with varying orientations and results in a heterogeneous structure with limited long-range order. As illustrated in Fig. 2. The results exhibited a strong correlation between the estimated and quantified surface area measurements along with the crystal diffraction angles; the Scherer equation is used to determine the crystallite size, which can be represented as follows[17]

$$D = \frac{0.9\lambda}{\beta \cos\theta} \quad (1)$$

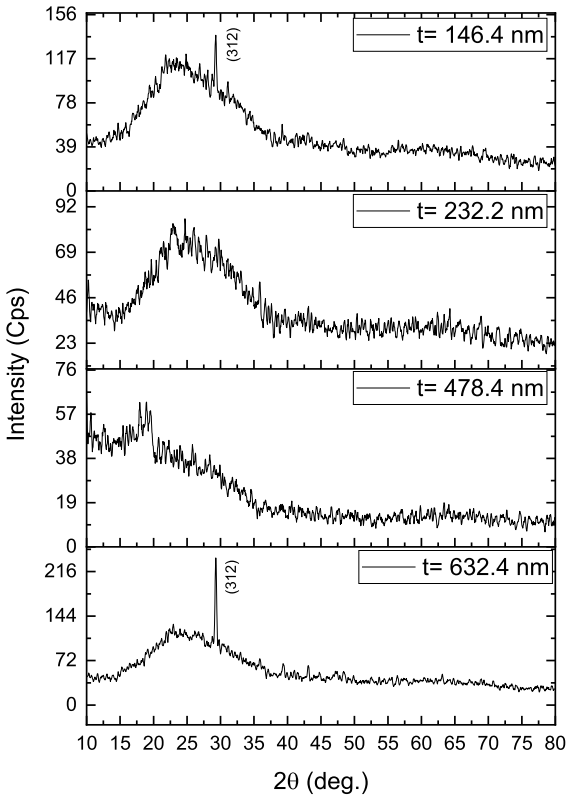

Fig. 2. X-ray diffraction patterns of copper phthalocyanine thin films produced on a glass substrate at ambient temperature via thermal evaporation process for thicknesses of 146.4, 232.2, 478.4, and 632.4 nm.

Where D The crystalline size of the crystallite, with $\lambda = 1.54059$ Å representing the wavelength of the utilised X-rays, is denoted by β: Expansion of the diffraction line assessed at half of its peak intensity in radians and the angle of diffraction (θ). Table 1 presents the structural properties of CuPc films, indicating that an increase in thin film thickness correlates with a rise in crystallite size, attributed to columnar growth influenced by both film thickness and deposition rate.

At 232.2 nm in thickness, the peak intensity of the diffraction slightly decreases and becomes broader, indicating that the islands start to coalesce and form a denser layer. At this thickness, microstrain and smaller crystallites are to be expected due to the merging of the initially isolated domains, leading to partial crystallinity loss and structural defects. This agrees with the findings of AFM, wherein both roughness and grain size decreased significantly, justifying the production of smoother and more uniform surface, For the 478.4 nm-thick film, the intensity of the XRD peak remains low with a wider profile, which may be attributed to columnar grain formation and enhanced lattice defects. Grain growth in the vertical direction and microstrain lead to broadening of the diffraction peaks and reduction in intensity. Such behavior has been found to be corresponding to AFM data showing increased surface roughness and RMS, reflecting non-homogeneous grain structure and higher defect density at intermediate thickness. Maximum thickness (632.4 nm) is the point at which the diffraction peak for the (312) plane becomes sharper and significantly more intense, indicating higher crystallinity, lower lattice strain, and formation of a preferred texture (texture). This is due to the greater deposition thickness-induced reorganization and recrystallization of grains, in which the material accumulation available brings higher atomic rearrangement and lateral growth. These findings by AFM also conform to this trend as the surface comprises bigger but even grains with reduced roughness, which is an indication of the transition from vertical to lateral growth of grains. To calculate the microstrain (ϵ) from the XRD data in the table you sent, we use the following simplified form of the Williamson–Hall equation:[18]

$$\varepsilon = \frac{\beta \cos\theta}{4} \tag{2}$$

where β is the FWHM in radians and θ is the Bragg angle. The decrease in ϵ with increasing film thickness indicates reduced lattice imperfections and improved crystallinity.

The results in Table 1 exhibit a progressive increase in the crystallite size (D) with film thickness. This is attributed to the higher mobility and surface diffusion of CuPc molecules during film deposition that facilitates the coalescence of small grains to form large crystallites as the deposition continues. At greater thicknesses, the density of nucleation is lower, and thus the growth of crystallites that are already present is favored compared to the formation of new nuclei. Consequently, grains are larger and more regular, and the crystallinity is enhanced through the decrease of lattice defects. Furthermore, the reduction of full width at half maximum (FWHM) values with thickness supports this result, since smaller diffraction peaks directly correspond to larger crysta.

Table 1. Results acquired from X-ray diffraction for copper phthalocyanine films of varying thicknesses.

Thicknesses (nm)	2θ Deg.	FWHM Deg.	D (nm)	ε	hkl
146.4	29.25	0.2945	27.94763	1.24×10^{-3}	312
632.4	29.3149	0.2	41.15894	8.5×10^{-4}	312

Atomic force microscopy analysis

The roughness of the material was calculated by monitoring the roughness indices Sq and Sa, as well as the maximum peak height. The surface parameters include the mean roughness (Sa), the root mean square roughness (Sq), the shape of the histogram peaks, and other robust properties. As verified in the calculated areas, the mean roughness (Sa) is the average height. Sa is generally used to describe the roughness of machined surfaces. It helps detect general variations in peak characteristics and track the current production process. The root mean square roughness (Sq) represents the square root of the surface height distribution. The evolution of grain size, root mean square (RMS), and surface roughness (Sa) with the growing thickness of the film indicates that the growth mechanism of the film varies significantly during the deposition. The surface at the lowest thickness (146.4 nm) has a large grain size (275.1 nm) and high roughness values (RMS = 169.1 nm, Sa = 145.4 nm). This is attributed to the initial growth phase, where separated islands are formed owing to the poor diffusion of adatoms on the substrate surface. Island growth mode (Volmer–Weber type) accounts for the formation of big and irregular grains with a rough surface topography. Upon increasing the film thickness to 232.2 nm, the separated islands begin to merge and form a more continuous and uniform layer. This alteration results in an extraordinary decrease in grain size (23.56 nm) and surface roughness (RMS = 80.19 nm, Sa = 72.28 nm). The islands' coalescence fills the gaps and minimizes the surface irregularities, resulting in a smoother surface. With further thickness increase up to 478.4 nm, the film grows in columns, with the grains starting to grow vertically. This stage is characterized by a recrystallization process that increases grain size (35.77 nm) and enhances both RMS (169.2 nm) and roughness (145.2 nm) values due to the accumulation of grains of different orientations and heights. Surprisingly, for the largest thickness (632.4 nm), both RMS and roughness decrease again (RMS = 114.5 nm, Sa = 95.83 nm) despite the moderate growth of grain size (66.7 nm). This can be explained by grain reorganization and lateral growth, whereby the deposited material fills surface vacancies and smoothes the topography. Enhanced atomic mobility and surface diffusion at higher thickness promote better surface uniformity and a denser film structure. Consequently, the final film is of relatively smoother and more even surface compared to the intermediate thickness, indicating a transition from vertical to lateral growth and partial re-crystallization of the surface,[19,20] as shown in Table 2 and Figs. 3 to 6.

UV-visible analysis

CuPc films thermally evaporated yield a distinct trend in the absorption spectrum as thickness varies with a well-defined increase in intensity of absorption at all wavelengths due to the longer optical path of the light wave within the film and a higher number of absorbing molecules. Characteristic absorption bands of CuPc molecules can also be readily observed: the B-band in the ultraviolet (UV) region (approximately 330–380 nm) for the σ to σ^* transitions, and the Q-band in the visible region (approximately 600–700

Table 2. Values of (Avg.D, RMS (Sq), Roughness (Sa) of (CuPc) thin film of the temperature (R.T) and values of thickness (t = 146.4, 232.2, 478.4 and 632.4) nm.

Thickness (nm)	Avg.D	RMS (Sq)nm	Roughness (Sa)nm
146.4	275.1	169.1	145.4
232.2	23.56	80.19	72.28
478.4	35.77	169.2	145.2
632.4	66.70	114.5	95.83

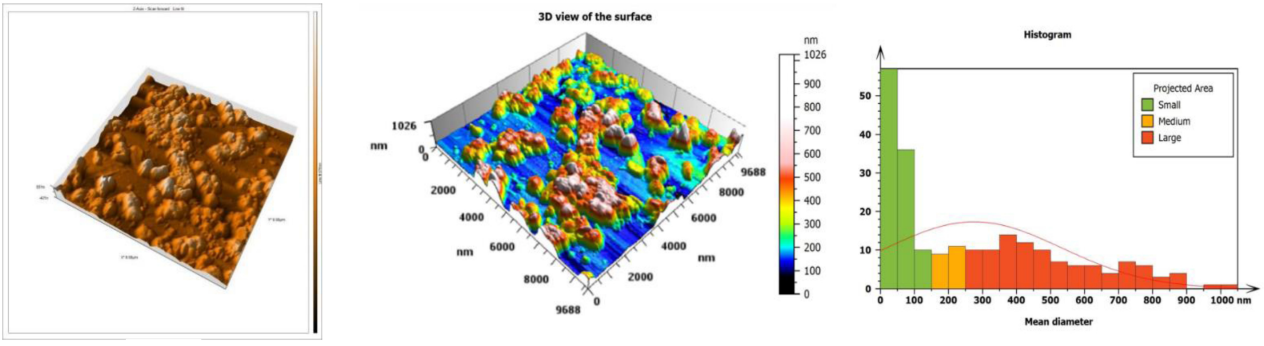

(a) (b) (c)

Fig. 3. AFM analysis for CuPc thin film (a) 2D image, (b) 3D image, and (c) granularity distribution diagrams at a thickness of 146.4 nm.

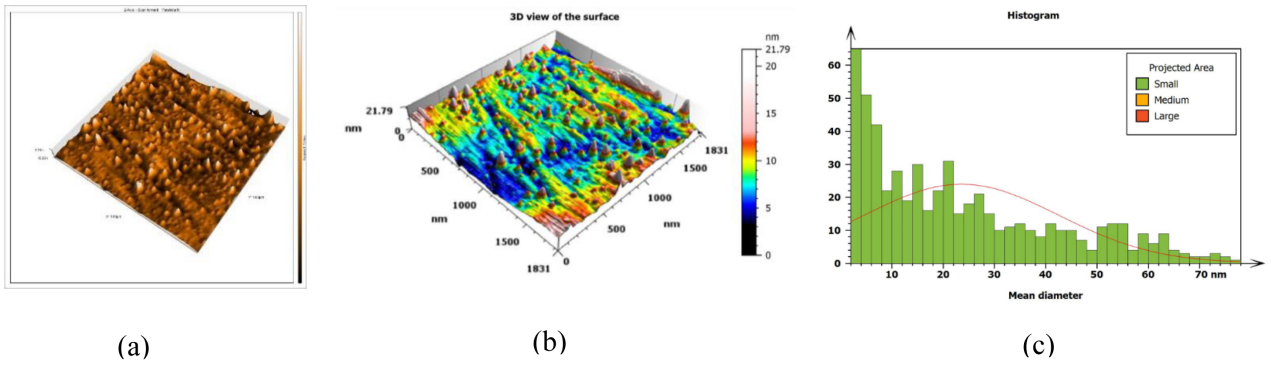

Fig. 4. AFM analysis for CuPc thin film (a) 2D image, (b) 3D image, and (c) granularity distribution diagrams at a thickness of 232.2 nm.

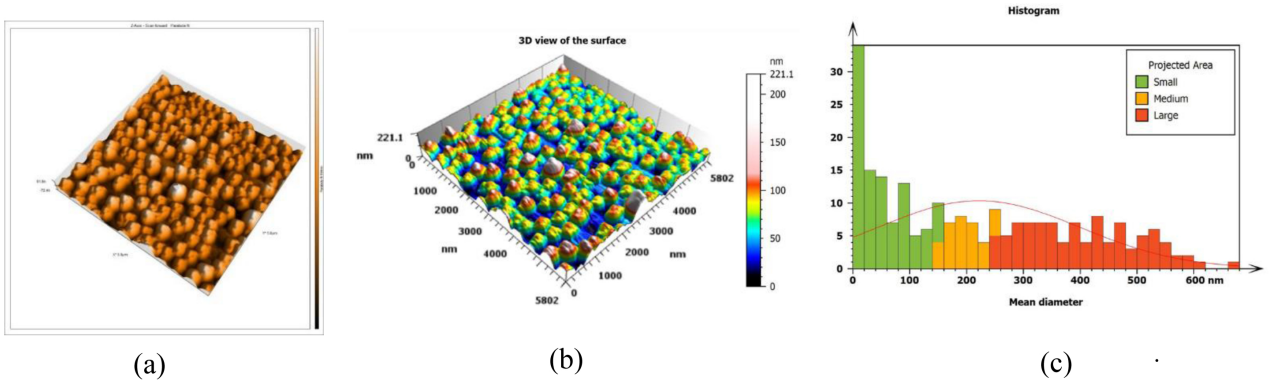

Fig. 5. AFM analysis for CuPc thin film (a) 2D image, (b) 3D image, and (c) granularity distribution diagrams at a thickness of 478.4 nm.

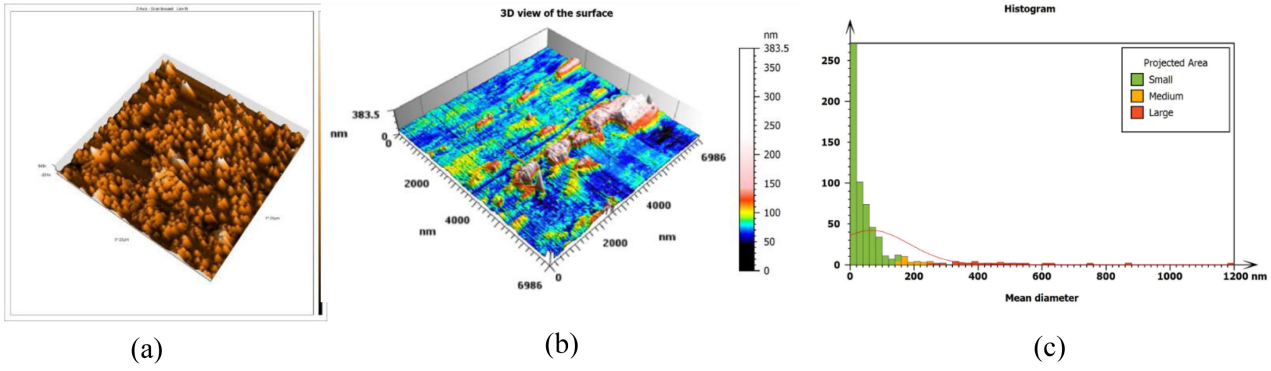

Fig. 6. AFM analysis for CuPc thin film (a) 2D image, (b) 3D image, and (c) granularity distribution diagrams at a thickness of 632.4 nm.

nm) as a result of electron transitions from the π orbital to the π^* orbital. With increasing thickness, red-shift of the Q band to longer wavelengths and considerable broadening of the peaks are observed. It is due to increased molecular packing (π–π stacking) among the phthalocyanine units and increasing ordered crystal structures, leading to greater interaction among molecular orbitals and reduced electron transition energy. This behavior also indicates a shift in molecular orientation in the layer, since in thicker films molecules are more regularly packed, with greater surface roughness and light scattering, which also cause increased absorption background. Thus, an increase in thickness causes increased overall absorbance, and structural and electronic changes in the CuPc layer indicate increased molecular packing and development of the film crystal structure. As shown in Fig. 7. Photon energy ($h\upsilon$) vs. $(\alpha h\upsilon)^2$ is plotted as seen in Fig. 8. (a, b, c, and d). Extrapolating the straight line to the linear region of the dot scatter plot to the x-axis gives details of the band gap energy. The calculated band gap energies and thickness

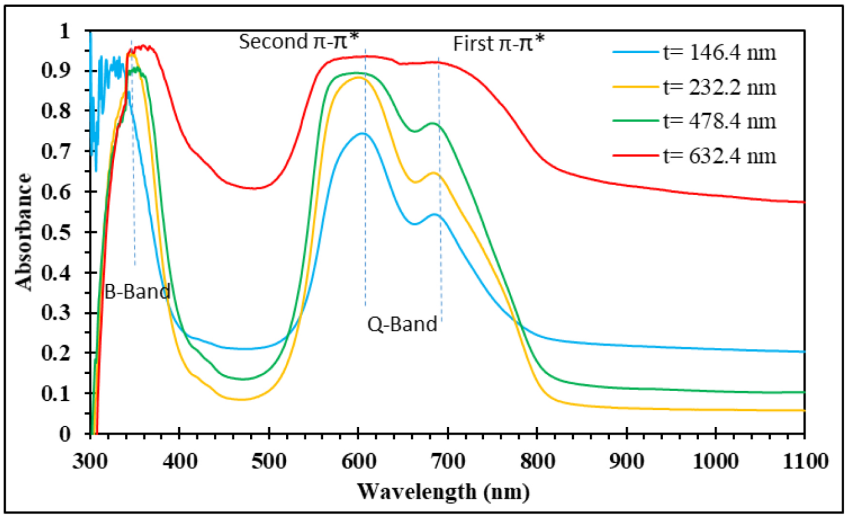

Fig. 7. Absorbance as a function of wavelength for CuPc thin films of varying thicknesses at ambient temperature.

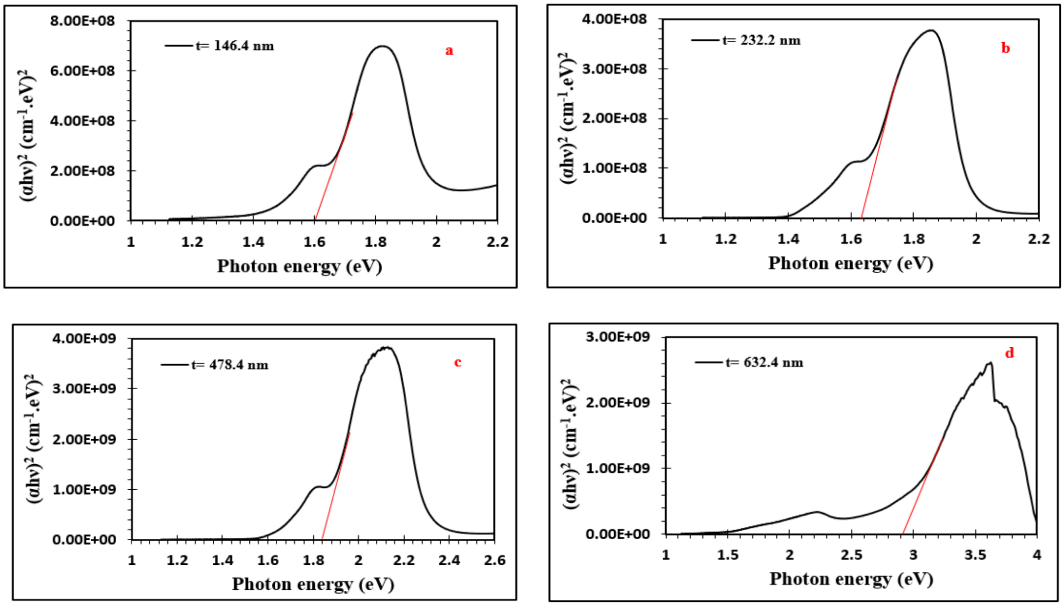

Fig. 8. The band gap of CuPc thin films deposited at various thicknesses at ambient temperature.

values for CuPc thin films are reported in Table 3. The formation of the energy gap with increasing thickness is attributed to the improvement of the crystal structure and increase in molecular order in the layer because of slow-layer growth during thermal evaporation. In very thin films, the molecules are highly disordered in the early growth phases and are beset by many surface deformations and defects, causing local defect states within the energy gap that reduce its effective magnitude. With higher thickness, more ordered layers are formed and interfacial defects are reduced and these local states disappear by and by, resulting in an effective broadening of the calculated energy gap. Greater thickness also tends to introduce the change in molecular stacking (π–π stacking), in which the molecules will stack in a more orderly fashion (from random to directed stacking). This reduces the overlap of π orbitals between molecules, and thus the electronic interaction between them is reduced. This widens the gap between the HOMO and LUMO levels and generates an increased energy gap. The internal stress effects and optical density variations in thicker layers may also contribute to the modification of the electronic structure of the material to create a higher energy gap than the one found for thin films. As shown in Table 3. The band gaps and thin film thickness of CuPc thin films

Table 3. The band gaps and thin film thickness of CuPc thin films.

Film thickness (nm)	E_g (eV)
146.4	1.6
232.2	1.63
478.4	1.82
632.4	2.9

I-V characteristics

An investigation was conducted on the current-voltage (I-V) properties at a temperature of 30 °C. The applied voltage varied from -5 V to +5 V, with increments of 0.1 mV at an area of 1 cm. The net photocurrent is determined by deducting the dark current from the measured photocurrent as shown in Eq. (3)[21]

$$I_{ph} = I_{light} - I_{dark} \tag{3}$$

Where I_{ph} is the illumination current, P is the incident luminous power, and A is the detector area.

Given that the dark current is significantly less than the photocurrent. The contact electrode is essential for effectively converting photoelectrons in CuPc thin films into the electrode. Fig. 9. illustrates the current-voltage (I-V) properties of CuPc films under dark conditions and when subjected to 625 nm light irradiation (with an intensity of less than 38.2 mW/cm^2). The I-V characteristics of CuPc thin films at different thicknesses demonstrate a linear correlation between current and the applied voltage. As the thickness of the thin layers increases, the current levels also rise, but for the thin film with a thickness of 478.4 nm, the current decreases. Suggesting that there were no resistance fluctuations during operation. Furthermore, the current observed under ultraviolet light is significantly greater than that observed in the absence of light (dark current). This phenomenon can be attributed to the generation of a higher number of charge carriers when exposed to ultraviolet light.

The response parameters, specific detection and quantum efficiency of the optical detector were calculated using the Eqs. (4) to (6)[21] as shown in Table 4.

$$R = \frac{I_{ph}}{PA} \tag{4}$$

$$D^* = \frac{R.\sqrt{A}}{\sqrt{2qI_D}} \tag{5}$$

$$EQE = \frac{I/q}{P/h\nu} \tag{6}$$

Photoresponse characteristics of the CuPc optical detector, including responsivity (R), specific

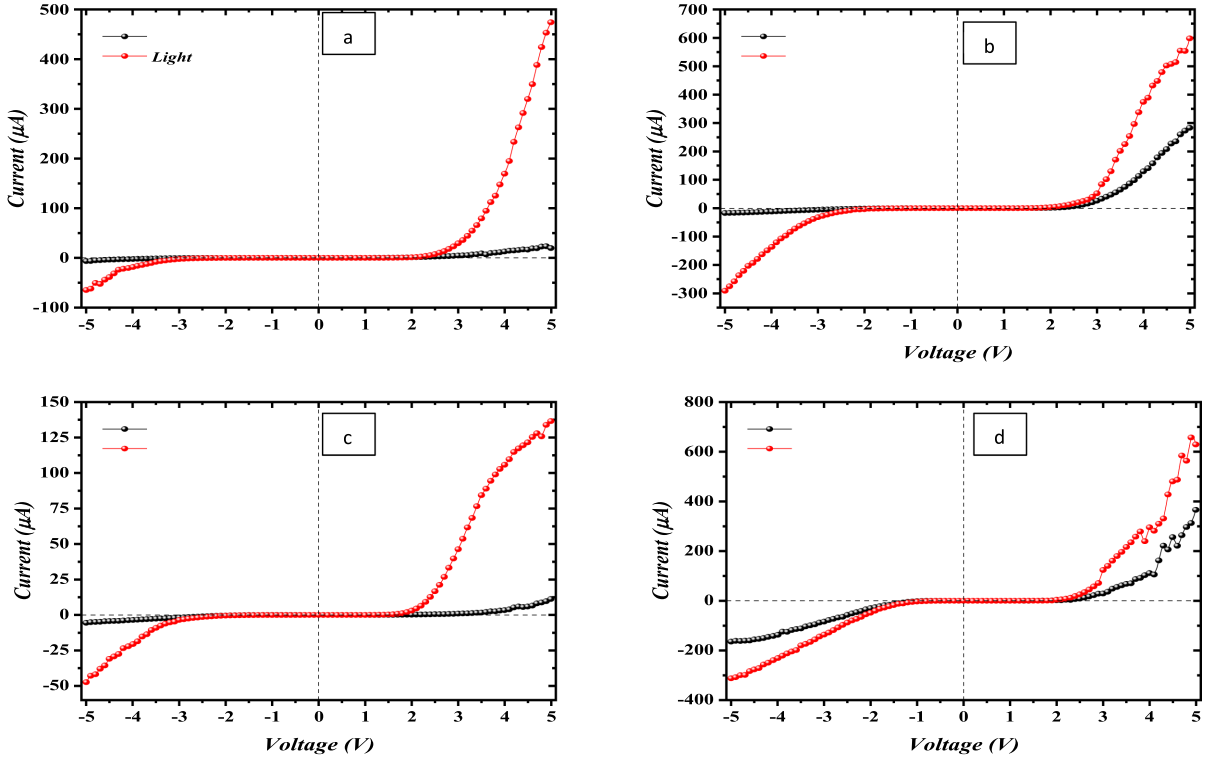

Fig. 9. Current-voltage characteristics for (a) 146.4, (b) 232.2, (c) 478.4 and (d) 632.4 nm sample under dark and illuminated states.

Table 4. Parameters of photo detector CuPc thin film with 625 nm for different thickness.

Thickness (nm)	Responsivity (μA/mW) λ (625 nm)	Detectivity $\times 10^9$ (Jones) λ (625 nm)	EQE (%) (625 nm)	T_{rise} (sec.)	T_{fall} (sec.)
146.4	17.30	3.99	3.43	0.29	0.30
232.2	16.63	4.25	3.29	0.30	0.32
478.4	54.92	19.3	10.89	0.30	0.31
632.4	10.64	2.92	2.11	0.28	0.30

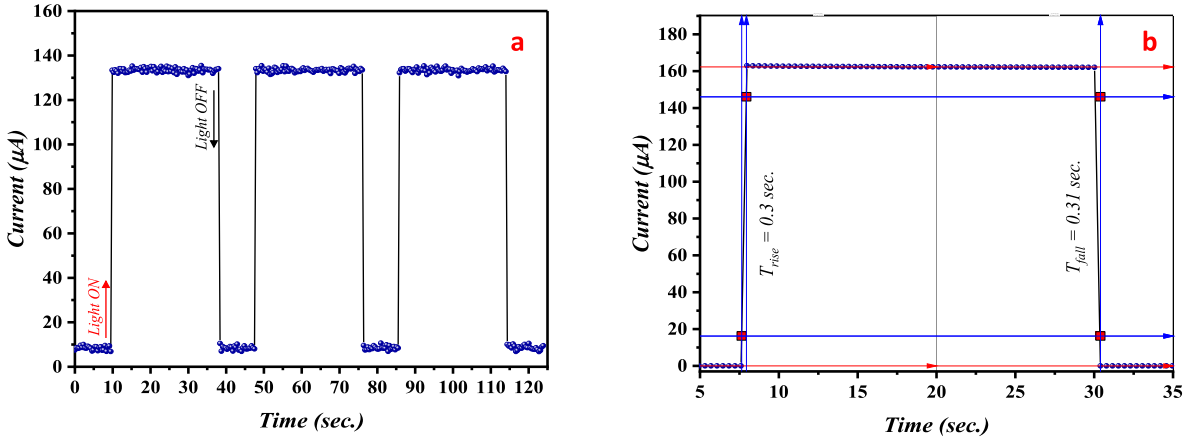

Fig. 10. (a) Time-dependent photocurrent response of CuPc photodetector; (b) Peak photocurrent of different light on-off cycles with thickness 146.4 nm.

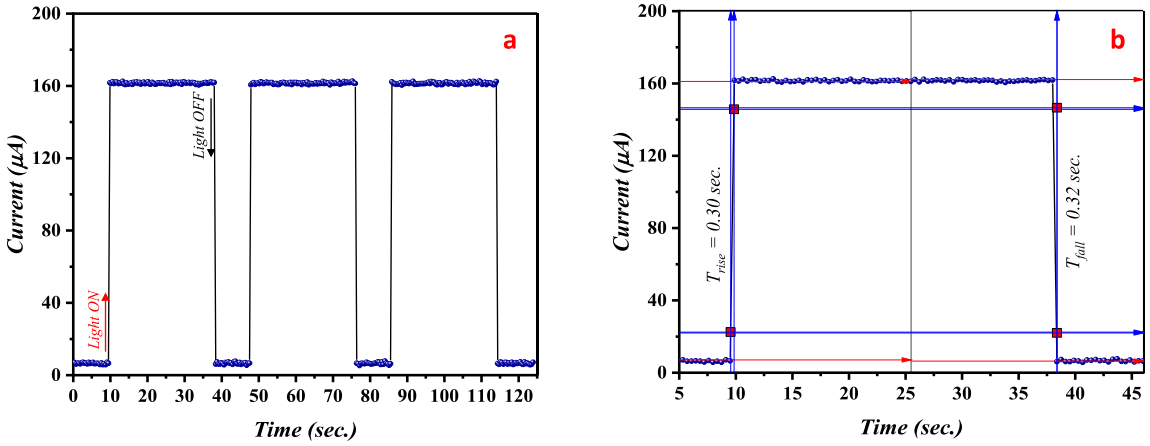

Fig. 11. (a) Time-dependent photocurrent response of CuPc photodetector; (b) Peak photocurrent of different light on-off cycles with thickness 232.2 nm.

detectivity (D*), and external quantum efficiency (EQE), were measured as a function of film thickness and correlated with surface morphology results of AFM analysis. As seen in Table 4, all of the response parameters were to a large degree dependent on the film thickness, with the best performance at 478.4 nm. At very high thickness, detectivity and responsivity increased considerably to 54.92 μA/mW and 1.93 $\times$ 10^{10} Jones, respectively, while the EQE reached as high as 10.89%. The AFM results showed that the film at 478.4 nm exhibited a denser and more even surface with lower average roughness and uniform grains spread evenly over the surface, indicating improved crystallinity and fewer defects. This surface topography is enhanced by optimization, boosting the charge carriers' mobility and minimizing recombination losses to enhance photoconductive efficiency. In the thinner films (146.4 and 232.2 nm), the AFM patterns revealed narrower grains and higher surface irregularities, which limit the transport of charges and decrease light absorption. Conversely, in the thicker films (632.4 nm), the surface exhibited higher coalescence and grain non-uniformity, leading to higher scattering and recombination, thus device performance decrease. The nearly equal rising and falling times (≈0.3 s) for all samples indicate that

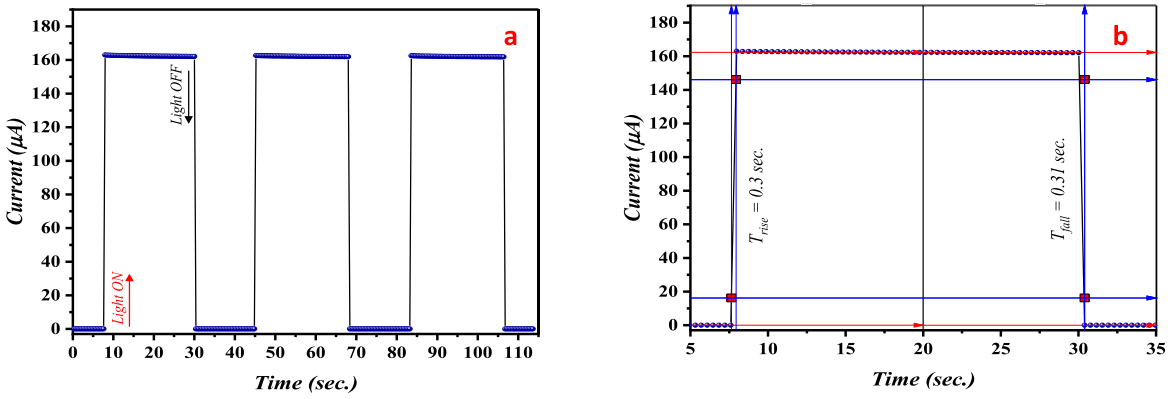

Fig. 12. (a) Time-dependent photocurrent response of CuPc photodetector; (b) Peak photocurrent of different light on-off cycles with thickness 478.4 nm.

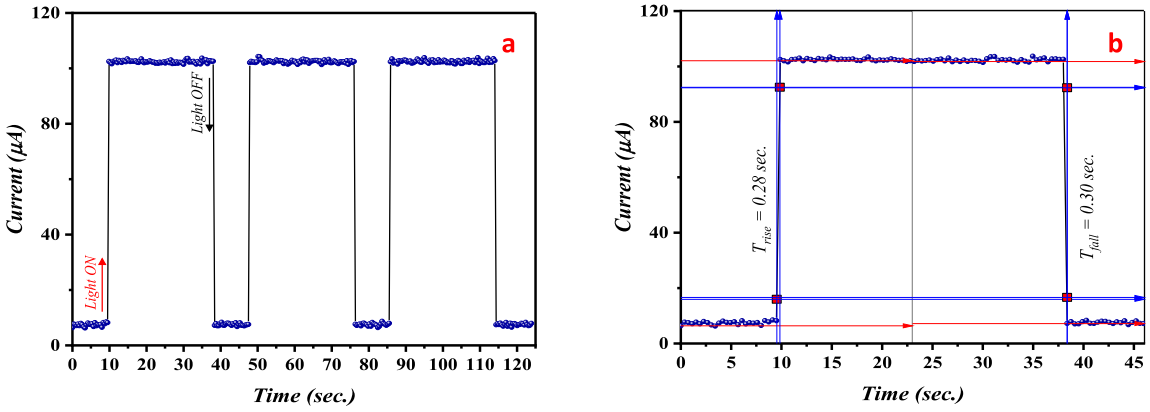

Fig. 13. (a) Time-dependent photocurrent response of CuPc photodetector; (b) Peak photocurrent of different light on-off cycles with thickness 632.4 nm.

there is a stable and reproducible photoresponse. Therefore, the complementarity of AFM and electrical measurements verifies that the CuPc film with thickness 478.4 nm provides a best-of-all-worlds situation among surface topography, optical absorption, and charge transport, resulting in optimal photodetector efficiency. As shown in Figs. 10 to 13.

Conclusion

This investigation experimentally established that CuPc thin film thickness is the governing parameter for their structural, morphological, optical, and electrical properties, which in turn control the overall performance of Schottky-type photodetectors. XRD analysis established that all the deposited CuPc films were polycrystalline with preferred (312) orientation, and increased film thickness was related to better crystallinity due to enhanced molecular ordering and decreased microstrain. AFM measurements showed that complex growth behavior was found with a transition from island-like to columnar and then to lateral growth at higher thicknesses, leading to more dense, smoother, and more homogeneous surfaces. Optical absorption measurements identified the typical Q and B bands of CuPc, and with rising thickness, the red shift and broadening were found, owing to greater π–π stacking and greater crystallite ordering. The optical band gap was observed to increase from 1.60 eV for the thinnest film to 2.92 eV for the thickest film, attributed to greater molecular packing and reduced defect density. Electrical measurements confirmed that the I–V characteristics of all CuPc films exhibited Schottky-type behavior, which established the existence of a potential barrier at the metal–semiconductor interface. Photodetector that was fabricated with a 478.4 nm-thick CuPc film exhibited the optimum photoresponse, whose responsivity (R), detectivity (D*), and external quantum efficiency (η) were 0.054 A/W, 1.93 $\times$ 10^{10} Jones, and 10.89%, respectively, under 625 nm illumination. The results are that this thickness has an optimal trade-off among surface morphology, light absorption, and charge transport. Finally, the thickness of

the CuPc film is of paramount importance in achieving optimal photoconductive performance and device stability. The findings exhibit the promising potential of thermally evaporated CuPc thin films as efficient, low-cost, and stable active layers for organic optoelectronics and photodetection technology.

Authors' declaration

- Conflicts of Interest: None.
- We hereby confirm that all the Figures and Tables in the manuscript are ours. Furthermore, any Figures and images that are not ours have been included with the necessary permission for republication, which is attached to the manuscript.
- No animal studies are present in the manuscript.
- No human studies are present in the manuscript.
- Ethical Clearance: The project was approved by the local ethical committee at University of Baghdad.

Authors' contributions statement

Z. H. A. Data curation, Writing–review and editing., S. Kh. Y. Conceptualization, Investigation, Methodology, M. K. K. Visualization, Writing – original

References

1. Hussein M T. Theoretical IR spectroscopic study of Copper Phthalocyanine (CuPc). NUCEJ. 1st Reg. Conf Eng Sci. 2008;11(2):303–306.
2. Esqueda M L, Vergara M E S, álvarez Bada J R, Salcedo R. CuPc: Effects of its doping and a study of its organic-semiconducting properties for application in flexible devices. Materials J. 2019 Jan;12(3):434–452. https://doi.org/10.3390/ma12030434.
3. Hassan Z M, Abdulameer A F. Structural and Morphological Properties of as-Deposited and Heat - Treated Composite (CuPc/Alq3) Thin Films. Iraqi J Sci. 2023;64(4):1717–1727. https://doi.org/10.24996/ijs.2023.64.4.13.
4. El-Nahass M M, Bahabri F S, AL Ghamdi A A, AL-Harbi S R. Structural and Transport Properties of Copper Phthalocyanine (CuPc) Thin Films. Egypt J Sol. 2002 Sep;25(2):307–321. https://doi.org/10.1016/j.tsf.2020.138250.
5. Yunfen S, Yang Z, Ying X. The Synthesis and Characterization of PANI-CuPc Organic Semiconductor Hybrid Material. Energy Procedia. 2012 Jan 1;17:1550–4. https://doi.org/10.1016/j.egypro.2012.02.280.
6. Mohammed RR, Hussein MT. Linear and Non-Linear Optical Properties for Organic Semiconductor (CuPc) Thin Films. Iraqi j phys. 2021 Mar 1;19(48):10–20. https://doi.org/10.30723/ijp.v19i48.639.
7. Chow AT. Natural organic matter under human-influenced environments: Implications for future environmental quality research. J. Environ. Qual. 2021 Nov;50(6):1347–50. https://doi.org/10.1002/jeq2.20301.
8. Elmas Duran N, Çapan I. A study on the effect of the macrocycle ring size and R-group chain length on the optical properties of the CuPc thin films. Indian J Phys. 2019 Jun 25;94(7):1061–70. https://doi.org/10.1007/s12648-019-01524-5.
9. Ejam AA, Wahhab NAA. Laser Irradiation Time Effect on the Optical Properties of Copper Phthalocyanine Solution. Neuro-Quantology. 2022 Mar 26;20(3):224–30. https://doi.org/10.14704/nq.2022.20.3.nq22064.
10. Madhavi J. Comparison of average crystallite size by X-ray peak broadening and illiamson–Hall and size–strain plots for VO2+ doped ZnS/CdS composite nanopowder. SN Applied Sciences. 2019 Oct 29;1(1509): https://doi.org/10.1007/s42452-019-1291-9.
11. Attia AA, M.M. Saadeldin, Soliman HS, A.-S. Gadallah, K. Sawaby. Structural and optical properties of p-quaterphenyl thin films and application in organic/inorganic photodiodes. Opt Mater. 2016 Oct 30;62:711–6. https://doi.org/10.1016/j.optmat.2016.10.046.
12. Alhiti LS, Jawad RA, Abd Alwaahed RA, Sobhi HM. Study of the Effect of Thin Layer Thickness on the Structural Properties of Copper Phthalocyanine (CuPc) Films Prepared by Vacuum Thermal Evaporation Method. Al-Kitab J Pure Sci. 2024 Apr 7;8(01):81–91. https://doi.org/10.32441/kjps.08.01.p8.
13. M Pirriera D, Puigdollers J, Voz C, Stella M, Bertomeu J, Alcubilla R. Optoelectronic properties of CuPc thin films deposited at different substrate temperatures. J Phys D Appl Phys. 2009 Jul;42(14):145102. https://doi.org/10.1088/0022-3727/42/14/145102.
14. Kolesov B A, Basova T V, Igumenov I K. Determination of the orientation of CuPc film by raman spectroscopy. Thin Solid Films. 1997 Jul;304(1):166–169. https://doi.org/10.1016/S0040-6090(97)00174-0.
15. Hongxia X, Zhongming W, Zhongming D, Wei X, Daoben Z. Facile method for fabrication of nanostructured CuPC thin films to enhance photocurrent generation. J Phys Chem C. 2008 Nov;112(50):19934–19938. https://doi.org/10.1021/jp8080673.
16. R. Marnadu, Chandrasekaran J, P. Vivek, V. Balasubramani, S. Maruthamuthu. Impact of Phase Transformation in WO_3Thin Films at Higher Temperature and its Compelling Interfacial Role in Cu/WO_3/p–Si Structured Schottky Barrier Diodes. J Phys Chem. 2019 May 24;234(2):355–79. https://doi.org/10.1515/zpch-2018-1289.
17. Abbas BH, Abdalameer NK, Mohammed RS. Synthesis of copper oxide nanostructures by Ar plasma jet and study of their structural and optical properties. Iraqi Journal of Science. 2024 Apr;30:1999–2006. https://doi.org/10.24996/ijs.2024.65.4.18.
18. Madhavi J. Comparison of average crystallite size by X-ray peak broadening and illiamson–Hall and size–strain plots for VO2+ doped ZnS/CdS composite nanopowder. SN Applied Sciences. 2019 Oct 29;1(1509). https://doi.org/10.1007/s42452-019-1291-9.
19. To TB, Almeida R, Ferreira SO, Reis FD. Roughness and correlations in the transition from island to film growth: Simulations and application to CdTe deposition. Applied Surf. Sci. 2021 Sep15;560:1–11. https://doi.org/10.1016/j.apsusc.2021.149946.
20. Sakthinathan S, Meenakshi GA, Vinothini S, Yu CL, Chen CL, Chiu TW, Vittayakorn N. A Review of Thin-Film Growth, Properties, Applications, and Future Prospects. MDPI. 2025 Feb19;13(2):1–41. https://doi.org/10.3390/pr13020587.
21. Ali H, Zhang Y, Tang J, Xu X. High-Responsivity Photodetection by a Self-Catalyzed Phase-Pure p-GaAs Nanowire. Small. 2018 Apr;14(17):1–9. https://doi.org/10.1002/smll.201704429.

تأثير سمك غشاء CuPc المُحضر بالتبخير الحراري على أداء الكاشف البصري

زينب حازم عبدالرحيم[1]، سمير خضر ياسين[1]، محمد خماس خلف[2]

[1] قسم الفيزياء، كلية علوم بنات، جامعة بغداد، بغداد، العراق
[2] هيئة البحث العلمي، بغداد، العراق

الخلاصة

فثالوسيانين النحاس (CuPc) شبه موصل يتميز بثبات كيميائي عالي، وامتصاص ضوئي عالي للضوء المرئي، وخصائص نقل شحنة ممتازة، ما يجعله مادة واعدة للأجهزة البصرية الإلكترونية وكاشفات الضوء. في هذه الدراسة، تم تنمية أغشية رقيقة من فثالوسيانين النحاس (CuPc) بسمك يتراوح بين 146.4 و632.4 نانومتر على ركائز زجاجية مُنظفة بالموجات فوق الصوتية عن طريق التبخير الحراري عند ضغط 2.2×10^{-5} تور. حُللت البنية والشكل والخصائص البصرية لدراسة تأثير السمك على الاستجابة الضوئية. كشف تحليل حيود الأشعة السينية أن الأغشية متعددة البلورات أحادية الميل، مع اتجاه مفضل (312). أظهرت صور المجهر الذري (AFM) زيادة في حجم الحبيبات مع السمك، وانخفاضًا في الخشونة عند زيادة السمك نتيجة زيادة كثافة السطح. أظهرت أطياف الامتصاص مناطق Q وB مميزة، ولوحظ ازدياد فجوة الطاقة من 1.60 إلى 2.92 إلكترون فولت مع زيادة السُمك. أظهرت منحنيات التيار-الجهد في الظلام والإضاءة سلوكًا من نوع شوتكي، مما يدل على وجود حاجز جهد عبر الوصلة بين المعدن وشبه الموصل، وهو المسؤول عن نقل الشحنة. كما أظهر جهاز الكشف الضوئي المصنوع من أغشية رقيقة من كربيد النحاس والكوبالت (CuPc) استجابة بصرية جيدة، حيث بلغت قيمة الكفاءة الكمية 10.89%، وقيمة الاستجابة 0.054 A/W، وقيمة الكاشفيه النوعية 10^9 جونز عند الإضاءة بطول موجة 625 نانومتر. تؤكد هذه النتائج أن أغشية كربيد النحاس والكوبالت تتميز بخصائص بصرية وكهربائية تعتمد على السُمك، وتُمثل آفاقًا واعدة لتطبيقات كاشف ضوئي من نوع شوتكي عالية الأداء ومستقرة.

الكلمات المفتاحية: مجهر القوة الذرية، فثالوسيانين النحاس، الترسيب الفيزيائي للبخار، الأشعة فوق البنفسجية -المرئية، ، حيود الأشعة السينية.